RESEARCH ARTICLE

The Ferrous Iron-Responsive BqsRS Two-Component System Activates Genes That Promote Cationic Stress Tolerance

Naomi N. Kreamer,[a] Flavia Costa,[a]* Dianne K. Newman[a,b,c]

Division of Biology and Biological Engineering,[a] Division of Geological and Planetary Sciences,[b] and Howard Hughes Medical Institute,[c] Caltech, Pasadena, California, USA

* Present address: Flavia Costa, Microbiology Department, University of Georgia, Athens, Georgia, USA.

ABSTRACT **The physiological resistance of pathogens to antimicrobial treatment is a severe problem in the context of chronic infections. For example, the mucus-filled lungs of cystic fibrosis (CF) patients are readily colonized by diverse antibiotic-resistant microorganisms, including *Pseudomonas aeruginosa*. Previously, we showed that bioavailable ferrous iron [Fe(II)] is present in CF sputum at all stages of infection and constitutes a significant portion of the iron pool at advanced stages of lung function decline [R. C. Hunter et al., mBio 4(4):e00557-13, 2013]. *P. aeruginosa*, a dominant CF pathogen, senses Fe(II) using a two-component signal transduction system, BqsRS, which is transcriptionally active in CF sputum [R. C. Hunter et al., mBio 4(4):e00557-13, 2013; N. N. Kreamer, J. C. Wilks, J. J. Marlow, M. L. Coleman, and D. K. Newman, J Bacteriol 194:1195–1204, 2012]. Here, we show that an RExxE motif in BqsS is required for BqsRS activation. Once Fe(II) is sensed, BqsR binds a tandem repeat DNA sequence, activating transcription. The BqsR regulon—defined through iterative bioinformatic predictions and experimental validation—includes several genes whose products are known to drive antibiotic resistance to aminoglycosides and polymyxins. Among them are genes encoding predicted determinants of polyamine transport and biosynthesis. Compared to the wild type, *bqsS* and *bqsR* deletion mutants are sensitive to high levels of Fe(II), produce less spermidine in high Fe(II), and are more sensitive to tobramycin and polymyxin B but not arsenate, chromate, or cefsulodin. BqsRS thus mediates a physiological response to Fe(II) that guards the cell against positively charged molecules but not negatively charged stressors. These results suggest Fe(II) is an important environmental signal that, via BqsRS, bolsters tolerance of a variety of cationic stressors, including clinically important antimicrobial agents.**

IMPORTANCE **Clearing chronic infections is challenging due to the physiological resistance of opportunistic pathogens to antibiotics. Effective treatments are hindered by a lack of understanding of how these organisms survive *in situ*. Fe(II) is typically present at micromolar levels in soils and sedimentary habitats, as well as in CF sputum. All *P. aeruginosa* strains possess a two-component system, BqsRS, that specifically senses extracellular Fe(II) at low micromolar concentrations. Our work shows that BqsRS protects the cell against cationic perturbations to the cell envelope as well as low pH and reduction potential (Eh), conditions under which Fe^{2+} is stable. Fe(II) can thus be understood as a proxy for a broader environmental state; the cellular response to its detection may help rationalize the resistance of *P. aeruginosa* to clinically important cationic antibiotics. This finding demonstrates the importance of considering environmental chemistry when exploring mechanisms of microbial survival in habitats that include the human body.**

Received 23 December 2014 **Accepted** 7 January 2015 **Published** 24 February 2015

Citation Kreamer NN, Costa F, Newman DK. 2015. The ferrous iron-responsive BqsRS two-component system activates genes that promote cationic stress tolerance. mBio 6(2): e02549-14. doi:10.1128/mBio.02549-14.

Editor B. Gillian Turgeon, Cornell University

Address correspondence to Dianne K. Newman, dkn@caltech.edu.

Iron is an essential trace element for most life forms, occupying key positions in diverse metalloenzymes, spanning those involved in energy-yielding reactions to those critical for cellular defense (1–3). In the context of infections, the iron requirement of pathogens has resulted in an evolutionary arms race between host and microbe to sequester and obtain iron, respectively (4). The outcome of the infection depends on who wins this race: for example, iron can promote the formation of biofilms, complex microbial structures that are physiologically resistant to common antibiotics (5–7). Iron commonly exists in one of two oxidation states: the oxidized form, ferric iron [Fe(III)]; or the reduced form, ferrous iron [Fe(II)]. Fe(III) predominates in oxic environments, whereas Fe(II) is more stable under hypoxic and/or reducing conditions, with its ionic form (Fe^{2+}) predominating at low pH and reduction potential (Eh) (8). While Fe(III) uptake systems have been the focus of most mechanistically oriented studies, growing attention has been placed on the importance of Fe(II) sensing and uptake by pathogens. For example, *Pseudomonas aeruginosa*, the opportunistic pathogen renowned for causing chronic pulmonary infections in CF patients, contains an Fe(II)-specific two-component system, BqsRS (9); *Haemophilus influenzae*, another respiratory tract pathogen, contains a different Fe(II)-responsive two-component system, FirRS (10).

Recently, we reported average per patient micromolar concen-

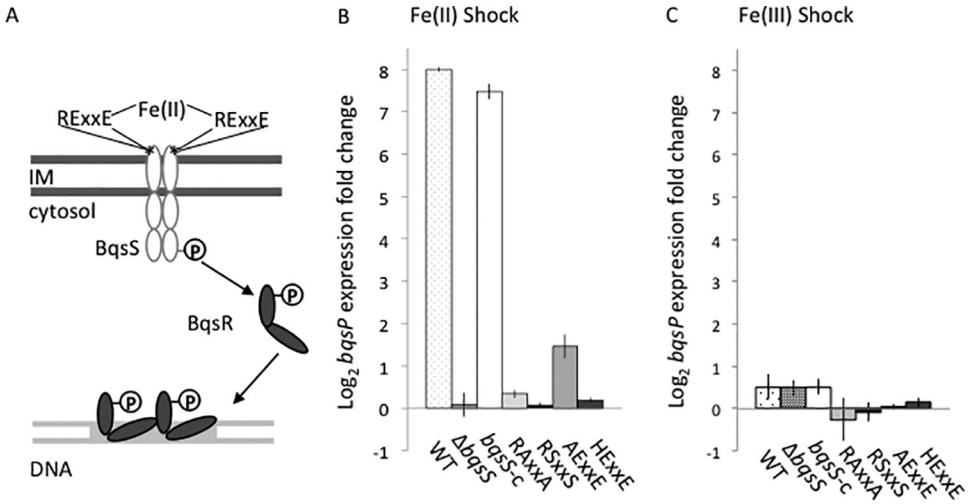

FIG 1 BqsS senses Fe(II) through the RExxE motif. (A) Model of BqsS activation by Fe(II) through the periplasmic RExxE motif and signal transduction to BqsR. This model is based on analogy to similar two-component systems (54). (B) Point mutations of the RExxE motif in BqsS show a decreased transcriptional response to Fe(II), suggesting that this may be the binding site of ferrous iron. From left to right, the bars show the $\log_2$-fold change in the *bqsP* (the first gene in the *bqs* operon) WT, Δ*bqsS*, *bqsS-c* (Δ*bqsS*::p*bqs-bqsS*), RAxxA (Δ*bqsS*::p*bqs*-RAxxA), RSxxS (Δ*bqsS*::p*bqs*-RSxxS), AExxE (Δ*bqsS*::p*bqs*-AExxE), and HExxE (Δ*bqsS*::p*bqs*-HExxE) strains. (C) Point mutations of the RExxE motif in BqsS show no transcriptional response to Fe(III). From left to right, the bars show the $\log_2$-fold change in the *bqsP* (the first gene in the *bqs* operon) WT, Δ*bqsS*, *bqsS-C* (Δ*bqsS*::p*bqs-bqsS*), RAxxA (Δ*bqsS*::p*bqs*-RAxxA), RSxxS (Δ*bqsS*::p*bqs*-RSxxS), AExxE (Δ*bqsS*::p*bqs*-AExxE), and HExxE (Δ*bqsS*::p*bqs*-HExxE) strains.

trations of Fe(II) in the mucus-filled environment of the lungs of cystic fibrosis (CF) patients (11). While the average value of sputum Fe(II) from patients at advanced stages of disease progression was ~40 μM, considerable variation existed between samples, with many presenting values greater than 100 μM and some over 200 μM. Fe(II), not Fe(III), correlated with severe lung function decline, with statistical significance comparable to or greater than that of other inflammatory indices (12, 13). While the presence of high Fe(II) concentrations in the lung may seem paradoxical given it is the site for oxygen exchange into the bloodstream (14), this finding is consistent with several studies that have found the CF mucus environment to contain hypoxic, if not anoxic, niches (15, 16). It is perhaps not coincidental that BqsRS-containing members of the *Pseudomonadaceae* are commonly found in soils and sediments (17), where Fe(II) can reach low micromolar concentrations (18). This environmental reservoir, together with the high Fe(II) concentrations found in sputum, may help contextualize why BqsRS is present in all sequenced strains of *P. aeruginosa* and why *bqsS* transcripts were detected in the majority of CF sputum samples tested (11).

With Fe(II) as a significant component of the CF lung environment and extracellular Fe(II) sensing predicted to be a conserved trait among diverse members of the *Pseudomonadaceae*, it is important to understand how *P. aeruginosa* responds to Fe(II). Other members of the *Pseudomonadaceae* (e.g., *Azotobacter vinelandii*) also contain BqsRS homologs, further motivating studies to better characterize this sensory system. *P. aeruginosa* has one of the largest regulatory networks of any bacterial species, which allows it to precisely control its response to a variety of environmental stimuli (19). The two-component system BqsRS was originally discovered as an effector of biofilm dissolution and quorum sensing (20); in a study using zebrafish embryos to screen two-component systems in *P. aeruginosa* for phenotypes, BqsS was shown to significantly impact the establishment of infection in the zebrafish host (21). When the trace metal concentration in the medium was controlled by chelation, we showed that BqsRS responds specifically to extracellular Fe(II) at concentrations exceeding 10 μM (9). However, while our previous study identified the *bqs* operon and a small number of BqsR-regulated genes, it did not define the BqsR regulon.

Because *bqsS* transcripts are detectable in CF sputum from patients with chronic *P. aeruginosa* infections, we wondered whether the BqsRS regulon might control factors that affect its adaptation to the Fe(II)-replete environment of CF sputum. We are broadly interested in understanding how *P. aeruginosa* survives under conditions relevant to the microenvironment of chronic infections, including anoxia and antimicrobial stressors. Here, we sought to gain insight into how BqsS senses Fe(II) and how BqsR controls gene transcription. We identified the BqsRS regulon through bioinformatic, genetic, and biochemical approaches and tested predicted phenotypes. This study expands our knowledge of how *P. aeruginosa* responds to Fe(II) and suggests that a common mechanism helps protect the cell against Fe(II) and other cationic stressors, including certain clinically relevant antibiotics.

RESULTS

Fe(II)-sensing residues. Under standard laboratory conditions, the BqsRS system is specifically sensitive to extracellular Fe(II) and not other dipositive cations (9). Multiple bacterial protein prediction programs (TMpred [22] and DAS [23]) predict the sensor kinase BqsS to be a two-pass transmembrane protein with a periplasmic region containing an RExxE motif (Fig. 1A). A similar motif is present in a variety of iron-binding proteins; an HExxE motif is found in the Fe(III)-sensing *Salmonella* PmrAB two-component system (24), and an RExxE motif is present in the yeast Ftr iron permease (25). To determine whether the RExxE motif is involved in Fe(II) sensing, we generated strains with substitutions in these residues in a Δ*bqsS* mutant background. Alleles

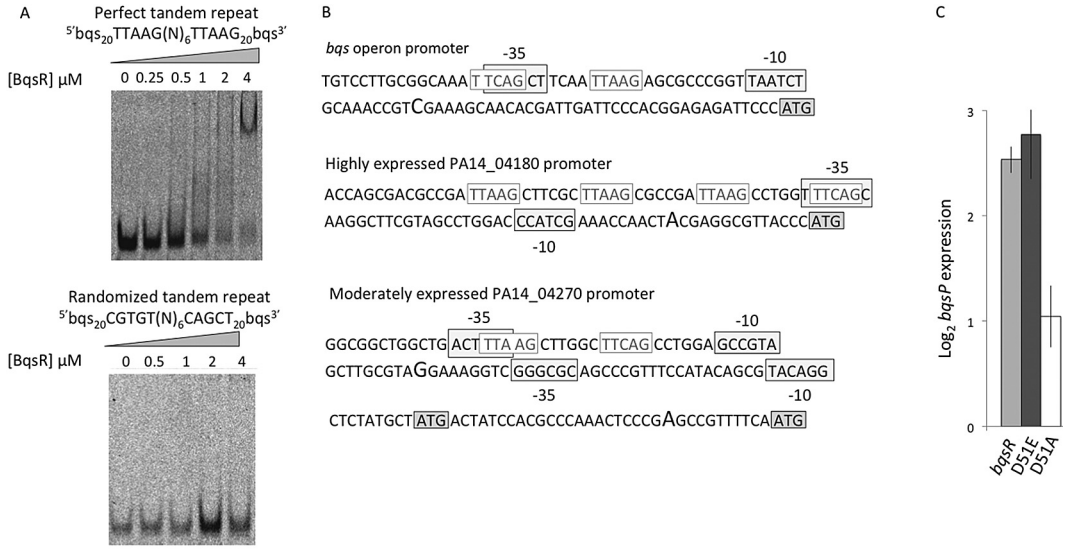

FIG 2 BqsR binds to a bioinformatically predicted tandem repeat that overlaps with the RNA polymerase binding site and appears to be activated by phosphorylation. (A) Gel shift assays demonstrate that BqsR binds to the specific tandem repeat TTAAG(N)$_6$TTAAG and within the same flanking DNA sequence does not bind to a randomized tandem repeat with the same binding energy. (B) By determining the transcription start site of three genes, *bqsP*, PA14_04180, and PA14_04270, that are upregulated to different degrees by cRACE, it is evident that the BqsR binding site overlaps with the RNA polymerase -35 binding site. The box shaded dark gray highlights the translation start site; the light gray box indicates the -10 and -35 RNA polymerase binding sites; the white box with gray letters shows the BqsR binding sites. (C) In the Δ*bqsR* background, *bqsR*, *bqsR*-D51E (a phosphomimic), or *bqsR*-D51A (cannot be phosphorylated) were inserted into the *glmS* locus under a constitutively active promoter. Cells were grown in 100 μM Fe(II) and 1 μM Fe(II), and transcription of *bqsP* was measured by qRT-PCR. The light-gray bar shows native *bqsR* activation by comparing expression between 100 μM Fe(II) and 1 μM Fe(II). The dark-gray bar shows expression of *bqsP* in *bqsR*-D51E in 1 μM Fe(II) to native *bqsR* grown in 1 μM Fe(II). The white bar compares expression of *bqsP* in *bqsR*-D51A in 100 μM Fe(II) to native *bqsR* grown in 1 μM Fe(II). Because the D51E phosphomimic mutant activation is similar to WT activation and D51A shows no upregulation, the phosphorylated form of BqsR likely binds DNA and activates transcription.

with substitutions in the RExxE residues were created and expressed from a chromosomal insertion at the *glmS* locus comprised of the *bqs* promoter and the *bqsS* gene. Activation of the BqsS variants in the presence of Fe(II) was measured by following the transcriptional response of *bqsP*, the first gene in the *bqs* operon, to 200 μM Fe(II) [here referred to as "Fe(II) shock"]. When the glutamates at positions 45 and 48 in BqsS were replaced with alanine (RAxxA) or serine (RSxxS), the transcriptional Fe(II) response was completely abolished. No change was seen in the levels of *bqsP* in these mutants, as for the Δ*bqsS* negative control (Fig. 1B). The arginine residue at position 44 is also critical: when this amino acid was replaced with alanine (AExxE), the Fe(II) shock response decreased by 98%, and when replaced with histidine (HExxE), the response was abolished. None of the site-directed mutants responded to Fe(III) shock (Fig. 1C). Fe(II) sensing thus appears to be mediated through the periplasmic RExxE motif in BqsS.

BqsR consensus DNA binding site. Having identified some of the key BqsS residues responsible for Fe(II) sensing, we sought to elucidate the BqsR DNA binding sequence. Previously, we performed a microarray experiment to determine whether there were genes uniquely upregulated in response to Fe(II) rather than Fe(III) or other dipositive cations (9). Not only did this experiment reveal the existence of the BqsRS system, it also alluded to genes that might be under its control. By inputting the 500-base-pair region upstream from the five most upregulated genes in the microarray (9) into the motif search program MEME (26), we generated putative consensus DNA binding motifs. BqsR belongs to the OmpR-like class of two-component systems, the most common type (27), in which the response regulator contains a phosphoreceiver domain and an effector domain. Members of this class of response regulators, such as OmpR and PhoP, are known to bind tandem repeat DNA sequences (28, 29). Accordingly, we reasoned that the most likely predicted BqsR DNA motif consisted of a 5-bp tandem repeat with 6 intervening nucleotides (see Fig. S1A in the supplemental material); we went on to test this biochemically and through iterative bioinformatic and transcriptional measurements.

Gel shift assays proved BqsR binds specifically to the MEME-predicted tandem repeat DNA sequence. Because the *bqs* operon is autoregulated (9), we incubated purified BqsR with a synthetic 60-bp DNA sequence from the *bqs* promoter region containing the tandem repeat. The native sequence contains one nucleotide substitution in the perfect tandem repeat consensus DNA sequence. Both the perfect tandem repeat (Fig. 2A) and the native tandem repeat (see Fig. S1B) showed decreased mobility with increasing protein concentrations on a native polyacrylamide gel, indicating BqsR-bound DNA. To ensure this was a sequence-specific shift, BqsR was incubated with the 56-bp sequence in the *tonB* promoter containing a Fur box (a palindromic sequence with no homology to the predicted BqsR box) with flanking 20-bp DNA regions. No shift was observed for the *tonB* sequence with the same concentrations of BqsR (see Fig. S1C). To determine whether the BqsR box was sufficient to bind BqsR, we placed the *bqs* tandem repeat into a *tonB* context by exchanging the flanking *bqs* 20-bp regions with those flanking the Fur box from the *tonB* promoter (see Fig. S1D). This hybrid sequence also showed a similar BqsR concentration-dependent decrease in mobility, signify-

ing that the *bqs* tandem repeat is sufficient for BqsR binding. As a final control, we randomized the *bqs* tandem repeat sequence while preserving its GC content (Fig. 2A); there was no shift with increasing BqsR concentration, demonstrating that the 5-bp *bqs* tandem repeat is necessary and sufficient for BqsR binding. While these experiments were performed without chemically phosphorylating BqsR (acetyl phosphate failed to generate stable phosphorylated BqsR), we would expect that phosphorylated BqsR would increase its affinity for DNA containing the BqsR box, as has been observed for other response regulators (30).

Promoter architecture and BqsR activation mechanism. To obtain a more finely resolved picture of how BqsR interacts with promoter regions—specifically, to identify where BqsR binds with respect to the RNA polymerase binding site—we performed rapid amplification of cDNA ends (cRACE) on three representative BqsR-regulated genes (PA14_04180, *bqs* operon, and PA14_04270) with a range of induced expression levels from high to low (Fig. 2B). Using the transcription start sites identified by cRACE, we could identify the -10 and -35 RNA polymerase binding sites. For both PA14_04180 and the *bqs* promoter, the -35 RNA polymerase binding site overlaps with one of the BqsR tandem repeat sites. PA14_04270 contains two transcription start sites, of which the most upstream site's -35 position also overlaps with the BqsR binding site.

Because the BqsR DNA binding site overlaps with the RNA polymerase binding site, we wondered whether BqsR acts as a classical transcriptional activator. Previously, it has been shown that transcription factor binding sites that overlap the -35 RNA polymerase sigma binding site can activate transcription by helping recruit RNA polymerase to the promoter (31). To test whether BqsR serves as an activator *in vivo*, we replaced the conserved phospho-acceptor aspartate with a glutamate to mimic a constitutively phosphorylated response regulator, or we changed the aspartate to an alanine to prevent the response regulator from being phosphorylated; this experimental design assumes functional conservation between BqsR and other two-component regulators at this residue (32–34). *bqsR* alleles containing one of these mutations were placed under the control of a constitutive weak promoter at a neutral site (35), in the Δ*bqsR* mutant background. The expression level of a BqsRS-regulated gene (*bqsP*) in the strain carrying the phosphomimic mutant should indicate the function of the activated BqsR, and its expression level in the nonphosphorylatable mutant should indicate the function of the unphosphorylated form. The D51E mutant is constitutively activated and, when grown in 1 μM Fe(II), shows transcript levels similar to those of wild-type (WT) cells grown in 100 μM Fe(II); the D51A mutant does not enhance *bqsP* expression under any condition (Fig. 2C). This suggests that BqsR is an activator when phosphorylated. Consistent with this interpretation, the Δ*bqsR* strain does not induce the BqsR regulon. Together, these *in vivo* data suggest that BqsRS is a classical two-component system, with the Fe(II) signal presumably causing BqsS to phosphorylate BqsR and phosphorylated BqsR binding DNA to activate a transcriptional response; this remains to be proven biochemically.

Predicted BqsR regulon. Having validated the predicted BqsR binding motif, we searched the genome to identify candidate BqsR-regulated genes using two strategies. First, we used a regular expression approach. We selected the most common variants of the *bqs* tandem repeat consensus sequences by eye from our initial position weight matrix (PWM) (see Fig. S1A in the supplemental material). A representative regular expression sequence was $TTAMG(N)_{4-8}TTAMG$, which assumed no preference for the nucleotides between the tandem repeat sequences (Fig. 3A). We then searched the intergenic regions of the PA14 genome for matches to these regular expressions using the Motif Search tool available on the *Pseudomonas* Genome Database (36). The final PWM (Fig. 3B) was reached through multiple rounds of generating new lists of potential BqsR-regulated genes, verifying new members of the regulon by reverse transcriptase quantitative PCR (qRT-PCR) and adding the upstream regions to the MEME input to generate a refined PWM (see Materials and Methods in the supplemental material). This PWM identified approximately 75 genes, while the regular expression approach identified 62 gene targets. Genes identified through both methods were annotated using information from a variety of databases (see Dataset S1 in the supplemental material) and classified by David (37) (Table 1). A subset of these were tested by qRT-PCR if they met one of three criteria: (i) found in both the regular expression approach and the PWM-based approach (Fig. 3C); (ii) present in a cluster of genes with similar function (Table 1); or (iii) had an E value of less than 50 from the PWM approach (see Dataset S1). This high E value was chosen to obtain the broadest possible set of putative BqsR-regulated genes.

All of the previously identified Fe(II)-responsive genes (9) showed BqsR-dependent upregulation with Fe(II) shock when tested by qRT-PCR. While some of these predicted genes appeared in our earlier microarray study (9), that study was performed only

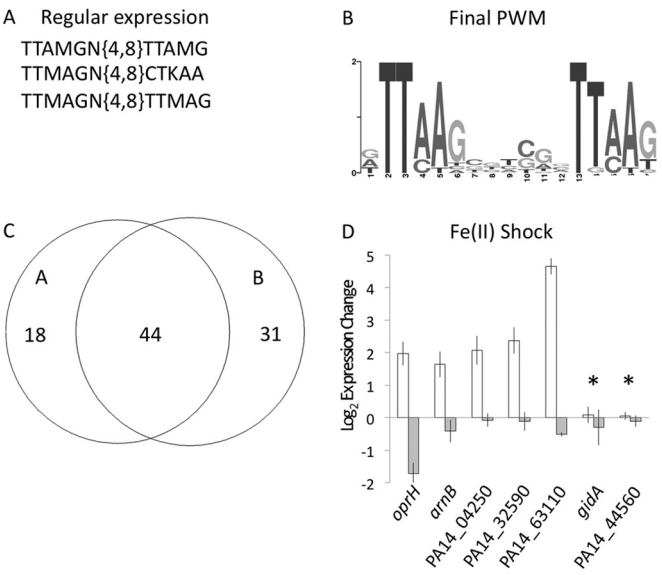

FIG 3 Bioinformatic predictions of the BqsR regulon. (A) Motifs reflecting the search parameters used to manually search (using regular expressions) the intergenic regions of the PA14 genome. (B) Final position-weight matrix based on genes with BqsR-dependent qRT-PCR-verified upregulation in high Fe(II) concentrations. (C) A Venn diagram depicting in circle A the number of genes predicted by the regular expression motif and in circle B the number of genes predicted through the qRT-PCR-generated PWM given in Dataset S1 in the supplemental material. There was substantial overlap between the proposed regulons of the regular expression PWM and the qRT-PCR-generated PWM. (D) qRT-PCR validation of 5 genes predicted to be BqsR regulated, *oprH*, *arnB*, PA14_04250, PA14_32590, and PA14_63110, with 2 negative controls (marked by *) without the BqsR tandem repeat, *gidA* and PA14_44560. White bars correspond to WT, gray bars to the Δ*bqsR* strain.

TABLE 1 Broad predicted functions of genes identified by either regular expression or the PWM approach based on homology of their gene products to known proteins and categorized by David

Function	No. of genes[a]	% annotation
Protease/hydrolase activity	15	8.6
Transposition, DNA metabolic process	3	1.7
(Poly)amine metabolism	4	2.3
Metal binding/hydrolase	14	8.0
Protein complex assembly	3	1.7
Outer membrane/envelope	6	3.4
Metabolism/regulation	50	28.7
RNA metabolic process	3	1.7
Signal transducer/two-component system	5	2.9
Membrane/transport	18	10.3
Redox/cofactor binding	11	6.3
ATPase/nucleotide binding	6	3.4
Transferase activity	7	4.0
Intracellular	3	1.7
23S RNA	4	2.3
Hypothetical	22	12.6

[a] Some genes fit into two categories.

in the WT in exponential phase, and the transcriptional response observed aggregated all direct and indirect effects of Fe(II) shock, not only those specific to BqsR. Five out of 12 newly predicted genes showed a BqsR-dependent Fe(II) shock response (Fig. 3D) in early exponential phase. Several of these genes have known or predicted functions involving cell stress resistance, polyamine biosynthesis/transport, or polymyxin resistance in *P. aeruginosa* strains. For example, *oprH*, a small outer membrane porin, is part of an operon containing the two-component system *phoPQ*, and all three genes are linked to polymyxin resistance (38). *oprH* is thought to stabilize the outer membrane, while *phoPQ* is upregulated by phosphate and Mg^{2+} limitation and contributes to resistance to polymyxins among other cationic antimicrobials (38, 39). *arnB* is the first gene of the operon *arnBCADTEF*, which together synthesize an aminoarabinose derivative covalently attached to lipid A, preventing electrostatic interaction of the polymyxin amine groups with the phosphates in the lipopolysaccharide (LPS) (40). PA14_04220 through PA14_04250 form an operon with structure and functional homology similar to those of the *potABCD* operon, a known spermidine/putrescine transporter (41). Finally, PA14_63110 is in an operon with PA14_63120, PA14_63130, and *pmrAB*, as confirmed by RT-PCR (see Fig. S2). PA14_63110 and PA14_63120 are predicted spermidine synthesis genes (42), and *pmrAB*, while unresponsive to Fe(III) in *P. aeruginosa* (unlike *Salmonella enterica* serovar Typhimurium) (43), has been shown to regulate genes that partially overlap the *phoPQ* regulon (44). PmrAB has also been shown to be involved in polymyxin resistance (44).

RNA-Seq. Because our qRT-PCR analysis and previous microarray study (9) were limited in scope (i.e., focused on particular genes under a single condition), we performed an RNA-Seq experiment to identify a broader set of BqsR-regulated genes and validate our bioinformatics predictions. For this experiment, we compared the WT to the Δ*bqsR* strain grown anaerobically in Fe-limited conditions until deep stationary phase, when quorum sensing is active (validated by measuring rhamnolipid production) (45), and subsequently shocked with 200 μM Fe(II). We expected that some genes under this condition might be coregulated by quorum-sensing regulators, which we would have missed in our earlier experiments. We analyzed the RNA-Seq data in multiple ways: by calculating the reads per kilobase per million reads mapped (RPKM) for each gene and sRNA in the genome (see Dataset S2) and by calculating this value for each predicted transcription unit as defined by Wurtzel et al. (46) (see Dataset S3). Genes or transcriptional units that showed 2-fold-higher expression in the WT strain than in the mutant strain under the iron shock condition and had a false discovery rate (FDR) value less than 0.01 (47) were considered to be differentially expressed in a BqsR-dependent manner.

The regular expression approach predicted 10/29 of the transcriptional units upregulated by BqsR in the RNA-Seq data (Fig. 3A), and the PWM predicted 11/29 (Fig. 3B), together accounting for 38% of the transcriptional units upregulated by BqsR in the RNA-Seq data. The functional annotation tool of the David suite identified several categories among the genes upregulated in our RNA-Seq data set: metabolism/regulation (30%), membrane (14%), unclassified (11%), protease/protein metabolism (10%), (poly)amine metabolism (8%), hypothetical (8%), metal binding (6%), localization (5%), outer membrane (4%), and redox (4%). We note that growth conditions impact the expression of the BqsR regulon. For example, qRT-PCR data showed that PA14_04250 has BqsR-dependent upregulation in early exponential phase but not in deep stationary phase; in contrast, *napE* is expressed in deep stationary but not in early exponential phase. Thus, the list of BqsR-regulated genes presented in Datasets S2 and S3 in the supplemental material likely represents a subset of the genes under its control.

Phenotypic response to Fe(II). Because much of the BqsR regulon is consistently upregulated upon Fe(II) exposure, this allowed us to identify phenotypes potentially under BqsRS control. Our first prediction was that BqsRS promotes cell tolerance of high Fe(II) levels. To test this, we compared the growth of the WT, Δ*bqsR*, and Δ*bqsS* strains in minimal medium under conditions in which BqsRS is inactive [5 μM Fe(II)] and conditions in which BqsRS is active [100 μM Fe(II)] (9). In the presence of low iron [5 μM Fe(II)], the strains grew similarly, whereas at high iron [100 μM Fe(II)], the Δ*bqsR* and Δ*bqsS* mutants showed significant growth defects compared to the WT (Fig. 4A). Complementation restored WT growth (see Fig. S3A in the supplemental material). The growth defect was also relieved by the addition of ferrozine, an Fe(II) chelator (Fig. 4B).

A striking aspect of the BqsR regulon is that many of its genes are predicted to play a role in polyamine biosynthesis and transport. For instance, decarboxylation of *S*-adenosylmethionine is predicted to be catalyzed by PA14_63110, and, subsequently, an amine group from *S*-adenosyl-L-methioninamine is transferred to putrescine by PA14_63120 to form spermidine. Transposon mutants of members of this operon, PA14_63110, PA14_63120, and *pmrA*, also show a moderate growth defect in high Fe(II) concentrations (see Fig. S3B). As mentioned previously, PA14_04220 through PA14_04250 are predicted to encode a spermidine/putrescine-specific transporter (48), and the PA14_04190 through PA14_04210 operon (induced in the RNA-Seq experiment) is also predicted by COG (49) to encode a polyamine transporter. Given that PA14_63110 and PA14_63120 homologs in *P. aeruginosa* PAO1 have been shown to promote outer membrane stability (50), we hypothesized that spermidine might protect the cell from anaerobic Fe(II) toxicity by electrostatically repelling the ferrous ion from the cell surface and intracellular

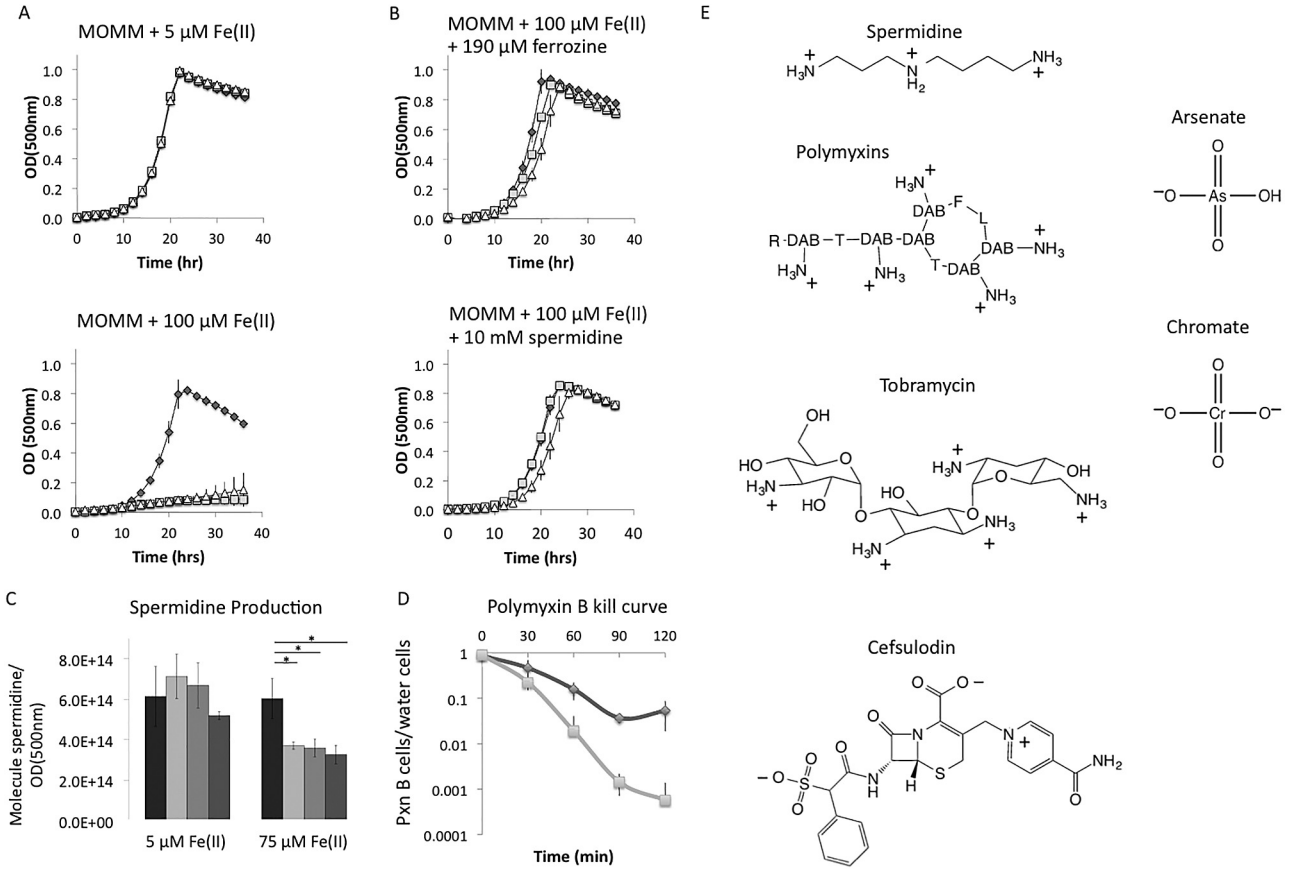

FIG 4 Physiological defects in deletion mutants in BqsRS both in growth deficiencies and increased antibiotic susceptibility. For growth in MOMM shown in panels A and B, diamonds are for the WT, squares are for the Δ*bqsR* mutant, and triangles are for the Δ*bqsS* mutant. (A) At 5 μM Fe(II), all strains grow like the WT. At 100 μM Fe(II), a condition where BqsRS is normally active, the deletion mutants show a deficiency in growth in both lag phase and final density. (B) When 190 μM ferrozine, which chelates 2 ferrozine:1 Fe(II), is added to 100 μM Fe(II), leaving ~5 μM free Fe, the growth defect is abolished. Exogenous addition of 10 mM spermidine can also rescue the growth defect. (C) BqsR upregulates genes in both spermidine biosynthesis and transport. Spermidine production was measured by HPLC and reported in molecules of spermidine/OD_{500}. The bars show spermidine production, from left to right, of the WT, Δ*bqsR*, Δ*bqsS*, and Δ*bqsRS* strains in 5 μM and 75 μM Fe(II). In high Fe(II), the deletion mutants produce significantly less spermidine. (D) Polymyxin B kill curves show percent survival of cells grown in 75 μM Fe(II) treated with polymyxin B over 2 h. The Δ*bqsR* mutant shown in light gray survived an order of magnitude less than the WT, shown in dark gray. (E) The structure of compounds used in this study at pH 7.2. Cationic structures include spermidine, the general polymyxin structure, and tobramycin (an aminoglycoside). Anionic compounds shown are cefsulodin (a β-lactam), arsenate, and chromate.

components. Consistent with this hypothesis, the mutants' growth defect was partially rescued by exogenous addition of 5 mM spermidine (see Fig. S3C) and fully rescued by 10 mM spermidine (Fig. 4B). Whether other polyamines can provide similar protection remains to be determined.

Because exogenous spermidine protected the mutants, we reasoned that the *bqsR* and *bqsS* deletion mutants were deficient in spermidine production in the presence of high Fe(II) concentrations. High-performance liquid chromatography (HPLC) analysis of polyamine extracts taken from cell lysate showed that the mutants produced approximately 50 to 66% as much spermidine as the WT when grown in the presence of 75 μM Fe(II) (Fig. 4C), whereas no significant difference in spermidine production was observed between the WT and the Δ*bqsR*, Δ*bqsS*, and Δ*bqsRS* strains in 5 μM Fe(II). Interestingly, for the WT, the total amount of spermidine in the culture did not increase from the 5 μM to the 75 μM Fe(II) growth condition.

Previous studies have indicated that spermidine can protect *P. aeruginosa* from several classes of cationic antimicrobials (42, 50). Additionally, BqsR-upregulated genes, such as *pmrAB*, *arnB*, *oprH*, and *phoPQ*, have been demonstrated to be involved in polymyxin resistance (19, 44). Accordingly, we tested susceptibility to polymyxin B by comparing killing curves of WT and Δ*bqsR* strains grown in 75 μM Fe(II) to late exponential phase (Fig. 4D). Typically, polymyxin survival assays are performed in aerobic conditions in rich medium, whereas our assays were performed anaerobically in minimal medium, where the doubling time is 4 to 10 times longer. This accounts for the increased time scale in the killing curve. After an hour of incubation at 37°C with 25 μg/ml polymyxin B, differences in WT and Δ*bqsR* mutant survival were observed. After 2 h, 3.7% of the WT survived, whereas only 0.14% of the Δ*bqsR* mutant survived. When complemented, the Δ*bqsR* strain behaved like the WT. Additionally, we observed a distinct morphological difference between WT and Δ*bqsR* colonies. The Δ*bqsR* colonies treated with polymyxin B varied greatly in size, and several satellite colonies could be seen (see Fig. S4A). We therefore counted the total number of colonies but kept track of the percentage of large and small. After 24 h of incubation, half of

TABLE 2 BqsRS guards against cationic but not anionic stressors[a]

Strain	MIC_{90}		Stressor	Stressor's charge
	5 μM Fe(II)	75 μM Fe(II)		
PA14	2 (μg/ml)	**1–2 (μg/ml)**	Tobramycin	+
Δ*bqsR* mutant	1 (μg/ml)	**0.25 (μg/ml)**	Tobramycin	+
PA14	256–512 (μg/ml)	8–16 (μg/ml)	Cefsulodin	−
Δ*bqsR* mutant	256 (μg/ml)	8 (μg/ml)	Cefsulodin	−
PA14	2–4 mM	2–4 mM	$HArO_4^-$	−
Δ*bqsR* mutant	2–4 mM	2–4 mM	$HArO_4^-$	−
PA14	250 μM	250–500 μM	CrO_4^-	−
Δ*bqsR* mutant	250 μM	250–500 μM	CrO_4^-	−

[a] MIC assays were performed for the WT and Δ*bqsR* strains under anaerobic conditions at two different iron concentrations for tobramycin, cefsulodin, arsenate, and chromate. Numbers in bold highlight where the absence of BqsR makes a difference.

the Δ*bqsR* colonies visible after 48 h were unobservable; counting solely colonies larger than a pinprick at this time point, we observed 0.07% survival for the Δ*bqsR* mutant compared to 3.0% survival in the WT (see Fig. S4B). Figure 4D shows survival calculated from final cell counts after 48 h of incubation. Δ*bqsR* mutant water-treated control and WT polymyxin B-treated cells showed consistent colony morphology after 24 h of incubation.

To test the hypothesis that BqsRS provides specific protection against diverse cationic stressors when activated by Fe(II), we performed MIC_{90} assays of both cationic and anionic stressors (Table 2). Due to differences in growth rate and lag phase between the WT and Δ*bqsR* strains in 75 μM Fe(II), we analyzed the MIC_{90} experiments at the time point where each strain achieved its maximum optical density in MOPS minimal medium (MOMM) without the stressor. Under these conditions, there was no MIC difference between the WT and Δ*bqsR* strains at 5 μM Fe(II) for any of the stressors, as expected, because this concentration is below the activation threshold for BqsRS. Only in the case of tobramycin, a cationic aminoglycoside (Fig. 4E), a significant difference could be seen at 75 μM Fe(II) (Table 2). When treated with tobramycin, 75 μM Fe(II), and 140 μM ferrozine (two ferrozines chelate one iron, leaving ~5 μM free Fe), both the Δ*bqsR* and WT strains had the same MIC (see Fig. S4C). Negatively charged stressors tested included cefsulodin (1 negative charge) (51), potassium chromate (2 negative charges), and sodium arsenate (1 or 2 negative charges; pK_a, 7.03). For both chromate and arsenate, the MIC was the same for both strains regardless of the Fe(II) concentration. For cefsulodin, the MIC differed depending on the Fe(II) concentration, a phenomenon that has been observed elsewhere (52); however, consistent with our hypothesis, BqsR did not affect the sensitivity level.

DISCUSSION

Characterizing the environment that pathogens encounter within the human host can help us understand their behavior. This principle is illustrated by connecting the output of the BqsRS regulatory system to the chemical context of CF sputum. Our research suggests that Fe(II) is an important environmental variable that *P. aeruginosa* senses through BqsRS, leading to a response that helps it cope not only with elevated Fe(II) concentrations but multiple cationic stressors within the CF lung environment.

The ability of BqsRS to specifically respond to Fe(II) is an interesting example of metal selectivity (9). Our results indicate that BqsS recognizes Fe(II) via the RExxE motif in its periplasmic domain, based on analogy to other Fe-sensing proteins. Although it is unusual for glutamates to prefer Fe(II) to Fe(III), the strongly positive arginine may tune the ligand environment to prefer the less positively charged Fe(II) over Fe(III). While PmrB from *S. typhimurium* senses Fe(III) rather than Fe(II) through a similar motif (HExxE), *Pseudomonas* PmrB does not bind Fe(III) (43). The *Pseudomonas* PmrB has a 32% amino acid similarity to *Salmonella*, yet the Fe(III)-binding domain in *Salmonella* strains is missing in *P. aeruginosa*'s PmrB. The *Salmonella* PmrB requires a distal serine in addition to the HExxE motif for Fe(III) binding (24). This suggests that other, less proximal residues may contribute to Fe(II) recognition by BqsS, particularly as arginine replacement by histidine or alanine is insufficient to convert BqsS to an Fe(III) sensor. HbpS from *Streptomyces reticuli* contains 8 ExxE Fe(II) binding sites, each with a required adjacent Arg or Lys (single point mutations of the R/K resulted in reduced activity even with 7 other intact binding sites) (53). This is consistent with the hypothesis that RExxE may directly bind Fe(II), and the R is a critical part of the Fe(II) binding event. The RExxE motif is just one strategy by which cells sense Fe(II): the FirRS system from *H. influenzae* utilizes a different motif, DYRED (10). Upon activation, two-component sensors can act as a kinase or a phosphatase to their cognate response regulators (54). BqsR prefers DNA binding sites that overlap RNA polymerase binding sites, suggesting that BqsR may help recruit RNA polymerase to promoter regions. As one of the few two-component systems for which the effector is known, BqsRS presents an attractive system for future biochemical studies to validate these predictions and explore the mechanisms of signal transduction.

Our primary goal in this study was to predict the biological response to extracellular Fe(II) mediated by BqsRS. Using iterative bioinformatic and experimental approaches to define BqsR regulon, we identified a set of approximately 100 genes potentially under BqsR control. Approximately a third of these genes encode proteins involved in stress tolerance, such as cation-binding, transport determinants, and lipopolysaccharide (LPS)-modulating proteins. Notably, several experimentally validated genes under BqsR control were annotated as playing a role in polyamine synthesis and transport. Polyamines, including spermidine, are present in all cells and environments (55) and are known to stabilize DNA and RNA, enhance translation and transcription, control porin-mediated transport, and increase the stability of LPS (41). A variety of metals are known to bind LPS (56), and dipositive ions modulate polymyxin sensitivity through interactions with LPS (57). Growing evidence has revealed that Fe(II) can be toxic under anaerobic conditions (58–60).

Because Fe(II) is thought to enter the cell through outer membrane porins (61, 62), that *bqs* mutants are particularly sensitive to high levels of Fe(II) yet can be rescued by exogenous spermidine is not surprising. The *bqs* mutants synthesize less spermidine than the WT, and while over 5 mM exogenous spermidine (a concentration higher than the reported intracellular spermidine concentration of 1 to 3 mM in bacteria [41]) is necessary to fully rescue these mutants, this can be rationalized by the fact that exogenous supplementation is different from endogenous production and that spermidine production is only one of several responses mediated by BqsRS that potentially helps confer resistance to Fe(II). *P. aeruginosa* possesses two different spermidine synthesis oper-

ons: *speDE* (bacterial in origin) and PA14_63110/PA14_63120 (archaeal in origin). The bacterial *S*-adenosylmethonine decarboxylase, *speD*, requires a dipositive cation (most commonly Mg^{2+}) for activity, whereas the archaeal homolog to PA14_63110 does not require a cation for activity (63). Because other metals may substitute for Mg^{2+} with reduced enzymatic activity (63, 64), we speculate that high Fe(II) perturbs intracellular metal homeostasis enough to reduce SpeD activity, accounting for the lower spermidine concentrations in the Δ*bqsR* and Δ*bqsS* mutants. At high Fe(II), BqsR induction of PA14_63110/PA14_63120 may compensate for SpeD's reduced activity, increasing the concentration of spermidine to homeostatic levels.

Given the plausible electrostatic mechanism underpinning polyamine-mediated resistance to Fe(II), we reasoned that BqsRS might also influence resistance to diverse cationic antibiotics but not anionic stressors. Previous studies have established that polyamines can mediate antibiotic resistance to cationic peptides, aminoglycosides, quinolones, and oxidative stress (42, 50, 65, 66). We show that *bqs* mutants exhibit increased sensitivity to tobramycin compared to the WT when stressed by high Fe(II) concentrations. In addition to the genes involved in spermidine production and transport, BqsRS upregulates other genes known to be involved in polymyxin resistance, such as *arnB* and *oprH*. Moreover, BqsRS activates *pmrAB* and *phoP*, which mediate polymyxin resistance in response to other environmental signals (limiting Mg^{2+}/Ca^{2+} and phosphate starvation, respectively [50, 67]). The polymyxin B killing curve demonstrates that the Δ*bqsR* strain is more sensitive than the WT in high Fe(II) conditions. Thus, BqsRS may be a master regulator under anoxic, Fe(II)-replete conditions, exerting indirect effects via modulating the expression of other regulatory systems. That BqsRS mediates a specific response to cationic stressors in the presence of high Fe(II) concentrations is supported by its lack of an effect on resistance to the negatively charged stressors cefsulodin, arsenate, and chromate.

Beyond mediating resistance to cationic antibiotics, BqsRS elicits a cellular response that is broadly relevant to survival in an environment where Fe(II) is a dominant parameter. Fe(II) is stable in a well-defined subset of environmental conditions spanning a range of acidic and reducing conditions (68). It is well known that such microhabitats are present in soil environments, which are also replete with diverse natural products that have antibiotic activities (69). While the evolutionary history of the BqsRS system is unknown, we note that pseudomonads (including *P. aeruginosa* isolates) are commonly found in soil environments (17). Sensing Fe(II) as proxy for these conditions may allow the cell to modulate its behavior accordingly. Consistent with this hypothesis, the BqsR regulon includes genes that protect the cell against pH and redox stress. For example, BqsRS upregulates *dsbB*, which helps control disulfide bond formation in the periplasm (70) and carbonic anhydrase, which promotes acid tolerance (71). Intriguingly, the most upregulated gene in the BqsR regulon, PA14_04180 (upregulated ~4,000-fold), is a predicted periplasmic bacterial oligonucleotide/oligosaccharide-binding (OB-fold) protein that likely binds positively charged molecules. This suggests that the cell may perceive a significant proportion of the Fe(II) pool in cationic form, consistent with the dominance of this species at low pH and Eh.

In summary, the connection between Fe(II) sensing and a response that broadly protects the cell against diverse cationic molecules—including clinically relevant antibiotics—reminds us of the importance of considering environmental chemistry when exploring mechanisms of microbial survival in habitats that include the human body. Typically, CF patients are first treated with aminoglycosides, beta-lactams, or fluoroquinolones. As lung function declines, polymyxins are employed as a last line of defense due to their harmful side effects (72). It is worth exploring whether a combination of aminoglycosides and polymyxins in conjunction with Fe(II) chelators or novel molecules targeting BqsRS could potentially be administered at lower concentrations, reducing side effects and increasing drug efficacy.

MATERIALS AND METHODS

Growth media. *Escherichia coli* was grown aerobically in LB supplemented with ampicillin 100 $\mu g \cdot ml^{-1}$ at 37°C. *P. aeruginosa* PA14 was grown both aerobically and anaerobically at 37°C in MOPS minimal medium (MOMM) in acid-washed glassware to ensure cells were Fe limited. The basic MOMM is composed of 40 mM succinate ($C_4H_4Na_2O_4 \cdot 6H_2O$), 9.3 mM NH_4Cl, 2.2 mM KH_2PO_4, 25 mM KNO_3, 25 mM $NaNO_3$, 25 mM MOPS, 25 mM NaMOPS (pH 7.2). Additionally, immediately prior to inoculation, 100 μM $CaCl_2$, 1 μM $(NH_4)_2Fe(SO_4)_2 \cdot 6H_2O$, 1 mM $MgSO_4$, and trace metals were added (73). All PA14 cultures were prepared by overnight inoculation of MOMM with the desired strains, with shaking aerobically at 37°C. Cultures were grown aerobically into exponential phase (optical density at 500 nm [OD_{500}] ≈ 0.4 to 0.6) in fresh MOMM and then grown anaerobically with 50 mM nitrate as the electron acceptor in a Coy chamber with an atmosphere of 80% N_2, 15% CO_2, and 5% H_2. For anaerobic growth curves, biological triplicates of the WT and the deletion mutants were incubated in MOMM with 5 μM or 100 μM Fe(II). Anaerobic cultures were also grown with MOMM and 100 μM Fe(II) supplemented with 190 μM ferrozine, 5 mM spermidine, or 10 mM spermidine.

Ferrozine assay. The Stookey method (74) was modified for the 96-well-plate format to detect Fe(II) concentration. All measured Fe concentrations were within 5% of the reported value.

Cloning methods. Please see the details provided in the supplemental material.

BqsR purification. His_6-BqsR was expressed heterologously in *E. coli*. BqsR was induced with 1 mM isopropyl-β-D-thiogalactopyranoside (IPTG) at exponential phase and shifted from 37°C to 16°C overnight. Cells washed twice with wash buffer (500 mM KCl, 20 mM imidazole, 10% glycerol, and 20 mM Tris [pH 8]). DNase (2.5 units $\cdot ml^{-1}$) lysate, 5 mM $MgSO_4$, and 130 μM $CaCl_2$ were added to the suspension. Cell lysate was loaded onto a HisTrap HP column (GE Healthcare). Column-bound BqsR was washed with 100 mM imidazole to remove contaminating proteins and eluted with 200 mM imidazole. BqsR was dialyzed in dialysis buffer (50% glycerol, 300 mM KCl, 40.1 mM K_2HPO_4, 9.9 mM KH_2PO_4 [pH 7.4]) and concentrated, and flash-frozen BqsR aliquots were stored at −80°C. These storage conditions reflect the fact that BqsR is an unstable protein. For further details, see the supplemental material.

Gel shift assays. Various concentrations of BqsR were incubated with 5 nM double-stranded DNA (synthesized and purified by integrated DNA Technologies (IDT); both strands 5′ labeled with Cy5) in reaction buffer (15 mM KCl, 10% glycerol, 1 mM $MgSO_4$, 50 mM, 40.1 mM K_2HPO_4, 9.9 mM KH_2PO_4 [pH 7.4]) for 20 min at room temperature and run on an 8% acrylamide gel (0.5× TBE, 29 acrylamide:1 bis-acrylamide [Bio-Rad]). Each of the given parameters were optimized to yield the cleanest gel shift, and yet some smearing remained despite these efforts, possibly influenced by the instability of BqsR. Attempts to chemically phosphorylate BqsR with acetyl-P to enhance binding affinity were unsuccessful, which is not unprecedented for two-component transcription factors (75). DNA was visualized with Storm 860 in fluorescence mode using the 635-nm excitation laser. For further details, see the supplemental material.

Transcription start site determination. cRACE was used as previously described (76). Briefly, total RNA was isolated from 20 ml Fe(II) shocked early exponential cells as described above. cDNA was generated using a

gene-specific primer. The cDNA was ligated to adaptor DNA (WNp210) with an inverted 3′ T. A nested PCR was performed and TOPO cloned and sequenced by Sanger sequencing. For further details, see the supplemental material.

Point mutation growth conditions. Aerobic cultures of *P. aeruginosa* PA14 complementation strains and point mutants were grown overnight in 5 ml MOMM. BqsR strains were inoculated into anaerobic 1 μM Fe(II) MOMM and 100 μM Fe(II) MoMM in triplicate. Anaerobic cultures were grown at 37°C until early exponential phase (Beckman Spec20 OD_{500} = 0.2) and harvested with 10 ml RNAprotect. BqsS strains were inoculated into 1 μM Fe(II) MOMM and shocked with 200 μM Fe(II) anaerobically and harvested with 10 ml RNAprotect.

Consensus sequence generation. To make an initial BqsR consensus DNA binding site prediction, the 500 bp upstream from the translation start site of the 5 most upregulated genes (*bqsP*, PA14_ 04180, PA14_ 04270, PA14_ 01240, and PA14_ 07070) discovered in an Fe(II)/Fe(III) shock microarray (9) were used as input sequences for the motif-finding program, MEME (version 4.9.0) (26). The MEME input parameters allowed for zero or one sequence repetition, and 3 motifs returned with 6 to 50 nucleotides per motif. This generated the position weight matrix (PWM) used as the basis for the gel shift assays (see the supplemental material). Several PWM were generated by adding the 500-bp upstream regions of newly qRT-PCR-verified BqsR-regulated genes to the list of MEME input sequences as the genes were identified. The final version of the PWM was generated with MEME (version 4.9.1). The MEME input parameters allowed for any number of sequence repetitions, 3 motifs returned with 6 to 50 nucleotides per motif, and the program searched the given strand only. For further details, see the supplemental material.

BqsR regulon prediction. For the regular expression searching, we identified variants by selecting the most common sequences by eye from our initial PWM (shown in Fig. S1A in the supplemental material). For example, in Fig. S1A, position four in the first pentamer shows the most common nucleotides are A and C. Accordingly, our first regular expression was designed with this preference in a tandem repeat orientation, including a variable-length linker region (assuming no nucleotide preference in this region). The second regular expression kept the same sequence preferences for the first pentamer but considered a palindromic structure. The last regular expression was designed as a tandem repeat, only in this case we varied the sequence to reflect the preference shown in the second pentamer in the initial PWM (i.e., positions 12 to 16). Using these regular expressions, we searched the intergenic regions of the *P. aeruginosa* UCBPP-PA14 genome to identify potential BqsR-regulated genes (see Dataset S1).

The PWMs were uploaded into the MAST (version 4.9.1) tool (26), with the upstream region database selected for the *P. aeruginosa* UCBPP-PA14 genome. The E value cutoff was set to 50, and each strand was treated separately since the motif is a tandem repeat (rather than a palindrome). Also, by searching the intergenic regions of the PA14 genome for the most common variants of the tandem repeat consensus sequence, assuming no preference for the 6 nucleotides between the tandem repeat sequences (regular expression), a list of potential BqsR-regulated genes were identified. These upstream regions were then analyzed by MEME and MAST to generate the most broadly predicted BqsR regulon. We deliberately cast a wide net in our search process in order to identify a large set of genes to consider in follow-up tests, recognizing that some may be false positives (see Dataset S1).

Fe(II) shock conditions. Triplicate aerobic cultures of *P. aeruginosa* WT-pMQ72 and Δ*bqsR*-pMQ72 were grown in MOMM and 100 $\mu g \cdot ml^{-1}$ gentamycin at 37°C for 36 h. Anaerobic cultures were inoculated with 1% inoculum in MOMM, 100 $\mu g \cdot ml^{-1}$ gentamycin, and 1% arabinose. For qRT-PCR, when the cells reached early exponential phase (OD_{500} = 0.2), RNAprotect was added before and after a 30-min 200 μM $(NH_4)_2Fe(SO_4)_2 \cdot 6H_2O$ shock to sample the "unshocked" and "shocked" states, respectively. For the RNA-Seq experiments, when the cells reached deep stationary phase (OD_{500} = 0.8), RNAprotect was added before and after a 30-min 200 μM $(NH_4)_2Fe(SO_4)_2 \cdot 6H_2O$ shock. We are confident that Fe(II) induces transcriptional changes, not the counterion, sulfate, because MOMM contains a background of 1 mM sulfate. Additionally, previous 100 μM shock experiments were done with either $FeCl_2$ or $(NH_4)_2Fe(SO_4)_2 \cdot 6H_2O$, and no difference in expression was seen (9).

BqsR regulon gene annotation and classification. Genes seen in bioinformatic predictions and in the RNA-Seq data were manually annotated from the database with the lowest E value over the largest portion of the gene as viewed on the *Pseudomonas* Genome Database (36). Databases used include COG (77), TIGRFAM (78), Pfam (79), CD (80), prk (81), and SMART (82). To cluster genes with similar annotations, David (37) was set to medium stringency with all possible input databases and terms selected.

RNA-Seq processing. An RNeasy kit (Qiagen) was used to isolate RNA, and the Ribo-Zero magnetic kit (epicenter) was used to deplete rRNA. The NEBNext mRNA Library prep kit for Illumina (NEB) was used to prepare cDNA libraries for sequencing. Libraries were sequenced on an Illumina HiSeq2500 with 15 million read sequencing depth at the Caltech Millard and Muriel Jacobs Genetics and Genomics Laboratory. To analyze the data, Trimmomatic version 0.32 (83) was used to trim the low-quality bases from the reads, with parameters set to LEADING:27 TRAILING:27 SLIDINGWINDOW:4:20 MINLEN:35. The trimmed reads were mapped to the genome using Bowtie 1.0.1 (84). SAMtools 0.1.19 (85) was used to sort the mapped reads. Read counts per gene or transcriptional unit were calculated using easyRNASeq (86), using .gff gene description files generated from the curated genome hosted by NCBI (NC_008463.1) (see Dataset S2), modified by the results of the single nucleotide resolution sequencing published by Wurtzel et al. (46) (see Dataset S3). Significance values for differential expression were determined (47) using Degust. The full data set is publicly available through the NCBI gene expression omnibus (GEO GSE65393).

mRNA isolation and qRT-PCR data analysis. mRNA was isolated using the RNeasy minikit (Qiagen) with optional on-column DNA digestion according to the manufacturer's instructions. Subsequently, the RNA was treated with TURBO DNA-free (Applied Biosystems), the rigorous treatment protocol. cDNA was generated using the extracted RNA as a template for an iScript (Bio-Rad) random-primed reverse transcriptase reaction by following the manufacturer's protocol. The cDNA was used as the template for quantitative PCR (real-time 7500 PCR Machine; Applied Biosystems) using iTaq universal SYBR green supermix (Bio-Rad). The elimination of genomic contamination was confirmed by running a qRT-PCR control plate with mRNA. Samples were assayed with 3 to 5 biological replicates. *recA* and *clpX* were used as endogenous controls (87). Fold changes were calculated using the threshold cycle ($\Delta\Delta C_T$) method (9). For further details, see the supplemental material.

Spermidine quantification by HPLC analysis. Biological triplicates of the WT, Δ*bqsR*, and Δ*bqsS* strains were prepared in MOMM, 5 mM arginine, and 5 mM methionine (MOMM-AA), with either 5 μM or 75 μM Fe(II), and grown as described above. Cultures were harvested at an OD_{500} of ≈0.7 and extracted. Suspensions with 1,3-diaminopropane added as an internal standard were dabsylated and analyzed by HPLC according to the protocol by Koski et al. (88). For further details, see the supplemental material.

Polymyxin B killing curve. Triplicate WT and Δ*bqsR* cultures were grown anaerobically in MOMM-AA and 75 μM Fe(II) to an OD_{500} of 0.7. Aliquots were incubated anaerobically with either water or 25 $\mu g \cdot ml^{-1}$ polymyxin B for 2 h. Samples were plated onto LB every 30 min. CFU counts were taken after 24 and 48 h, incubating aerobically at 37°C.

MIC assays. Cells were inoculated anaerobically in MOMM (pH 7.2) with tobramycin (0 to 8 μg/ml), cefsulodin (0 to 128 μg/ml), sodium arsenate (0 to 16 μg/ml), and potassium chromate (0 to 2 μg/ml) in either 5 μM Fe(II) or 75 μM Fe(II). MIC_{90} was calculated at the time each strain achieved maximum OD_{500} in wells with no antibiotic added. Each assay was performed with biological triplicates, and results were confirmed on two separate occasions.

Sequencing data accession number. The full sequencing data set can be found at the NCBI gene expression omnibus (GEO) under accession number GSE65393.

SUPPLEMENTAL MATERIAL

Supplemental material for this article may be found at http://mbio.asm.org/lookup/suppl/doi:10.1128/mBio.02549-14/-/DCSupplemental.

Text S1, PDF file, 0.1 MB.
Figure S1, TIF file, 2.8 MB.
Figure S2, TIF file, 2.8 MB.
Figure S3, TIF file, 2.8 MB.
Figure S4, TIF file, 2.8 MB.
Table S1, PDF file, 0.04 MB.
Table S2, PDF file, 0.1 MB.
Dataset S1, PDF file, 0.1 MB.
Dataset S2, PDF file, 0.1 MB.
Dataset S3, PDF file, 0.1 MB.

ACKNOWLEDGMENTS

We thank Megan Bergkessel, other members of the Newman laboratory, and anonymous reviewers for constructive comments on the manuscript.

This work was supported by grants to D.K.N. from the Howard Hughes Medical Institute (HHMI) and the National Heart, Lung, and Blood Institute of the National Institutes of Health (R01HL117328) and by the Millard and Muriel Jacobs Genetics and Genomics Laboratory at California Institute of Technology.

D.K.N. is an HHMI Investigator.

REFERENCES

1. **Kiley PJ, Beinert H.** 2003. The role of Fe-S proteins in sensing and regulation in bacteria. Curr Opin Microbiol **6:**181–185. http://dx.doi.org/10.1016/S1369-5274(03)00039-0.
2. **Fontecave M.** 2006. Iron-sulfur clusters: ever-expanding roles. Nat Chem Biol **2:**171–174. http://dx.doi.org/10.1038/nchembio0406-171.
3. **Lill R.** 2009. Function and biogenesis of iron-sulphur proteins. Nature **460:**831–838. http://dx.doi.org/10.1038/nature08301.
4. **Schalk I.** 2006. New insights on iron acquisition mechanisms in pathogenic *Pseudomonas*, p 1831–34. In Ramos J-L, Levesque R (ed), Pseudomonas. Springer, New York, NY.
5. **Banin E, Vasil ML, Greenberg EP.** 2005. Iron and *Pseudomonas aeruginosa* biofilm formation. Proc Natl Acad Sci U S A **102:**11076–11081. http://dx.doi.org/10.1073/pnas.0504266102.
6. **Patriquin GM, Banin E, Gilmour C, Tuchman R, Greenberg EP, Poole K.** 2008. Influence of quorum sensing and iron on twitching motility and biofilm formation in *Pseudomonas aeruginosa*. J Bacteriol **190:**662–671. http://dx.doi.org/10.1128/JB.01473-07.
7. **Mah TF, O'Toole GA.** 2001. Mechanisms of biofilm resistance to antimicrobial agents. Trends Microbiol **9:**34–39. http://dx.doi.org/10.1016/S0966-842X(00)01913-2.
8. **Stumm W, Lee GF.** 1961. Oxygenation of ferrous iron. Ind Eng Chem **53:**143–146. http://dx.doi.org/10.1021/ie50614a030.
9. **Kreamer NN, Wilks JC, Marlow JJ, Coleman ML, Newman DK.** 2012. BqsR/BqsS constitute a two-component system that senses extracellular Fe(II) in *Pseudomonas aeruginosa*. J Bacteriol **194:**1195–1204. http://dx.doi.org/10.1128/JB.05634-11.
10. **Steele KH, O'Connor LH, Burpo N, Kohler K, Johnston JW.** 2012. Characterization of a ferrous iron-responsive two-component system in nontypeable *Haemophilus influenzae*. J Bacteriol **194:**6162–6173. http://dx.doi.org/10.1128/JB.01465-12.
11. **Hunter RC, Asfour F, Dingemans J, Osuna BL, Samad T, Malfroot A, Cornelis P, Newman DK.** 2013. Ferrous iron is a significant component of bioavailable iron in cystic fibrosis airways. mBio **4**(4):pii: e00557-13. http://dx.doi.org/10.1128/mBio.00557-13.
12. **Mayer-Hamblett N, Aitken ML, Accurso FJ, Kronmal RA, Konstan MW, Burns JL, Sagel SD, Ramsey BW.** 2007. Association between pulmonary function and sputum biomarkers in cystic fibrosis. Am J Respir Crit Care Med **175:**822–828. http://dx.doi.org/10.1164/rccm.200609-1354OC.
13. **Kim J-S, Okamoto K, Rubin BK.** 2006. Pulmonary function is negatively correlated with sputum inflammatory markers and cough clearability in subjects with cystic fibrosis but not those with chronic bronchitis. Chest **129:**1148–1154. http://dx.doi.org/10.1378/chest.129.5.1148.
14. **Zeng A-, Kim E-J.** 2004. Iron availability, oxygen limitation, *Pseudomonas aeruginosa* and cystic fibrosis. Microbiology **150:**516–518. http://dx.doi.org/10.1099/mic.0.26933-0.
15. **Worlitzsch D, Tarran R, Ulrich M, Schwab U, Cekici A, Meyer KC, Birrer P, Bellon G, Berger J, Weiss T, Botzenhart K, Yankaskas JR, Randell S, Boucher RC, Döring G.** 2002. Effects of reduced mucus oxygen concentration in airway *Pseudomonas* infections of cystic fibrosis patients. J Clin Invest **109:**317–325. http://dx.doi.org/10.1172/JCI13870.
16. **Kolpen M, Kühl M, Bjarnsholt T, Moser C, Hansen CR, Liengaard L, Kharazmi A, Pressler T, Høiby N, Jensen PØ.** 2014. Nitrous oxide production in sputum from cystic fibrosis patients with chronic *Pseudomonas aeruginosa* lung infection. PLoS One **9:**e84353. http://dx.doi.org/10.1371/journal.pone.0084353.
17. **Green SK, Schroth MN, Cho JJ, Kominos SK, Vitanza-Jack VB.** 1974. Agricultural plants and soil as a reservoir for *Pseudomonas aeruginosa*. Appl Microbiol **28:**987–991.
18. **Gotoh S, Patrick WH.** 1974. Transformation of iron in a waterlogged soil as influenced by redox potential and pH. Soil Sci Soc Am J **38:**66–71. http://dx.doi.org/10.2136/sssaj1974.03615995003800010024x.
19. **Gooderham WJ, Hancock RE.** 2009. Regulation of virulence and antibiotic resistance by two-component regulatory systems in *Pseudomonas aeruginosa*. FEMS Microbiol Rev **33:**279–294. http://dx.doi.org/10.1111/j.1574-6976.2008.00135.x.
20. **Dong Y-H, Zhang X-F, An S-W, Xu J-L, Zhang L-H.** 2008. A novel two-component system BqsS-BqsR modulates quorum sensing-dependent biofilm decay in *Pseudomonas aeruginosa*. Commun Integr Biol **1:**88–96. http://dx.doi.org/10.4161/cib.1.1.6717.
21. **Chand NS, Lee JS, Clatworthy AE, Golas AJ, Smith RS, Hung DT.** 2011. The sensor kinase KinB regulates virulence in acute *Pseudomonas aeruginosa* infection. J Bacteriol **193:**2989–2999. http://dx.doi.org/10.1128/JB.01546-10.
22. **Hofmann K, Stoffel, W.** 1993. TMbase—a database of membrane spanning proteins segments. Biol Chem Hoppe Seyler **374:**166.
23. **Cserzö M, Wallin E, Simon I, von Heijne G, Elofsson A.** 1997. Prediction of transmembrane alpha-helices in prokaryotic membrane proteins: the dense alignment surface method. Protein Eng **10:**673–676. http://dx.doi.org/10.1093/protein/10.6.673.
24. **Wösten MM, Kox LF, Chamnongpol S, Soncini FC, Groisman EA.** 2000. A signal transduction system that responds to extracellular iron. Cell **103:**113–125. http://dx.doi.org/10.1016/S0092-8674(00)00092-1.
25. **Stearman R, Yuan DS, Yamaguchi-Iwai Y, Klausner RD, Dancis A.** 1996. A permease-oxidase complex involved in high-affinity iron uptake in yeast. Science **271:**1552–1557. http://dx.doi.org/10.1126/science.271.5255.1552.
26. **Bailey TL, Boden M, Buske FA, Frith M, Grant CE, Clementi L, Ren J, Li WW, Noble WS.** 2009. MEME suite: tools for motif discovery and searching. Nucleic Acids Res **37:**W202–W208. http://dx.doi.org/10.1093/nar/gkp335.
27. **Galperin MY.** 2010. Diversity of structure and function of response regulator output domains. Curr Opin Microbiol **13:**150–159. http://dx.doi.org/10.1016/j.mib.2010.01.005.
28. **Rampersaud A, Norioka S, Inouye M.** 1989. Characterization of OmpR binding sequences in the upstream region of the *ompF* promoter essential for transcriptional activation. J Biol Chem **264:**18693–18700.
29. **Blanco AG, Sola M, Gomis-Rüth FX, Coll M.** 2002. Tandem DNA recognition by PhoB, a two-component signal transduction transcriptional activator. Structure **10:**701–713. http://dx.doi.org/10.1016/S0969-2126(02)00761-X.
30. **Schaaf S, Bott M.** 2007. Target genes and DNA-binding sites of the response regulator PhoR from *Corynebacterium glutamicum*. J Bacteriol **189:**5002–5011. http://dx.doi.org/10.1128/JB.00121-07.
31. **Ghosh T, Bose D, Zhang X.** 2010. Mechanisms for activating bacterial RNA polymerase. FEMS Microbiol Rev **34:**611–627. http://dx.doi.org/10.1111/j.1574-6976.2010.00239.x.
32. **Gupte G, Woodward C, Stout V.** 1997. Isolation and characterization of *rcsB* mutations that affect colanic acid capsule synthesis in *Escherichia coli* K-12. J Bacteriol **179:**4328–4335.
33. **Lan C-Y, Igo MM.** 1998. Differential expression of the OmpF and OmpC porin proteins in *Escherichia coli* K-12 depends upon the level of active OmpR. J Bacteriol **180:**171–174.
34. **Klose KE, Weiss DS, Kustu S.** 1993. Glutamate at the site of phosphor-

ylation of nitrogen-regulatory protein NTRC mimics aspartyl-phosphate and activates the protein. J Mol Biol **232:**67–78. http://dx.doi.org/10.1006/jmbi.1993.1370.
35. **Choi K-H, Schweizer HP**. 2006. Mini-Tn7 insertion in bacteria with single attTn7 sites: example *Pseudomonas aeruginosa*. Nat Protoc **1:**153–161. http://dx.doi.org/10.1038/nprot.2006.24.
36. **Winsor GL, Lam DK, Fleming L, Lo R, Whiteside MD, Yu NY, Hancock RE, Brinkman FS**. 2011. *Pseudomonas* Genome Database: improved comparative analysis and population genomics capability for *Pseudomonas* genomes. Nucleic Acids Res **39:**D596–D600. http://dx.doi.org/10.1093/nar/gkq869.
37. **da Huang W, Sherman BT, Lempicki RA**. 2009. Systematic and integrative analysis of large gene lists using David bioinformatics resources. Nat Protoc **4:**44–57. http://dx.doi.org/10.1038/nprot.2008.211.
38. **Macfarlane EL, Kwasnicka A, Ochs MM, Hancock RE**. 1999. PhoP–PhoQ homologues in *Pseudomonas aeruginosa* regulate expression of the outer-membrane protein OprH and polymyxin B resistance. Mol Microbiol **34:**305–316. http://dx.doi.org/10.1046/j.1365-2958.1999.01600.x.
39. **Poole K**. 2005. Aminoglycoside resistance in *Pseudomonas aeruginosa*. Antimicrob Agents Chemother **49:**479–487. http://dx.doi.org/10.1128/AAC.49.2.479-487.2005.
40. **Miller AK, Brannon MK, Stevens L, Johansen HK, Selgrade SE, Miller SI, Høiby N, Moskowitz SM**. 2011. PhoQ mutations promote lipid A modification and polymyxin resistance of *Pseudomonas aeruginosa* found in colistin-treated cystic fibrosis patients. Antimicrob Agents Chemother **55:**5761–5769. http://dx.doi.org/10.1128/AAC.05391-11.
41. **Shah P, Swiatlo E**. 2008. A multifaceted role for polyamines in bacterial pathogens. Mol Microbiol **68:**4–16. http://dx.doi.org/10.1111/j.1365-2958.2008.06126.x.
42. **Johnson L, Mulcahy H, Kanevets U, Shi Y, Lewenza S**. 2012. Surface-localized spermidine protects the *Pseudomonas aeruginosa* outer membrane from antibiotic treatment and oxidative stress. J Bacteriol **194:**813–826. http://dx.doi.org/10.1128/JB.05230-11.
43. **McPhee JB, Lewenza S, Hancock RE**. 2003. Cationic antimicrobial peptides activate a two-component regulatory system, PmrA-PmrB, that regulates resistance to polymyxin B and cationic antimicrobial peptides in *Pseudomonas aeruginosa*. Mol Microbiol **50:**205–217. http://dx.doi.org/10.1046/j.1365-2958.2003.03673.x.
44. **Moskowitz SM, Ernst RK, Miller SI**. 2004. PmrAB, a two-component regulatory system of *Pseudomonas aeruginosa* that modulates resistance to cationic antimicrobial peptides and addition of aminoarabinose to lipid A. J Bacteriol **186:**575–579. http://dx.doi.org/10.1128/JB.186.2.575-579.2004.
45. **Parsek MR, Greenberg EP**. 2005. Sociomicrobiology: the connections between quorum sensing and biofilms. Trends Microbiol **13:**27–33. http://dx.doi.org/10.1016/j.tim.2004.11.007.
46. **Wurtzel O, Yoder-Himes DR, Han K, Dandekar AA, Edelheit S, Greenberg EP, Sorek R, Lory S**. 2012. The single-nucleotide resolution transcriptome of *Pseudomonas aeruginosa* grown in body temperature. PLoS Pathog **8:**e1002945. http://dx.doi.org/10.1371/journal.ppat.1002945.
47. **Law CW, Chen Y, Shi W, Smyth GK**. 2014. voom: precision weights unlock linear model analysis tools for RNA-seq read counts. Genome Biol **15:**R29. http://dx.doi.org/10.1186/gb-2014-15-2-r29.
48. **Yao X, Lu C-D**. 2014. Functional characterization of the *potRABCD* operon for spermine and spermidine uptake and regulation in *Staphylococcus aureus*. Curr Microbiol **69:**75–81. http://dx.doi.org/10.1007/s00284-014-0556-1.
49. **Tatusov RL, Koonin EV, Lipman DJ**. 1997. A genomic perspective on protein families. Science **278:**631–637. http://dx.doi.org/10.1126/science.278.5338.631.
50. **Kwon DH, Lu C-D**. 2006. Polyamines induce resistance to cationic peptide, aminoglycoside, and quinolone antibiotics in *Pseudomonas aeruginosa* PAO1. Antimicrob Agents Chemother **50:**1615–1622. http://dx.doi.org/10.1128/AAC.50.5.1615-1622.2006.
51. **Yotsuji A, Mitsuyama J, Hori R, Yasuda T, Saikawa I, Inoue M, Mitsuhashi S**. 1988. Outer membrane permeation of *Bacteroides fragilis* by cephalosporins. Antimicrob Agents Chemother **32:**1097–1099. http://dx.doi.org/10.1128/AAC.32.7.1097.
52. **Avery AM, Goddard HJ, Sumner ER, Avery SV**. 2004. Iron blocks the accumulation and activity of tetracyclines in bacteria. Antimicrob Agents Chemother **48:**1892–1894. http://dx.doi.org/10.1128/AAC.48.5.1892-1894.2004.
53. **Wedderhoff I, Kursula I, Groves MR, Ortiz de Orué Lucana D**. 2013. Iron binding at specific sites within the octameric HbpS protects *Streptomycetes* from iron-mediated oxidative stress. PLoS One **8:**e71579. http://dx.doi.org/10.1371/journal.pone.0071579.
54. **Laub MT, Goulian M**. 2007. Specificity in two-component signal transduction pathways. Annu Rev Genet **41:**121–145. http://dx.doi.org/10.1146/annurev.genet.41.042007.170548.
55. **Minguet EG, Vera-Sirera F, Marina A, Carbonell J, Blázquez MA**. 2008. Evolutionary diversification in polyamine biosynthesis. Mol Biol Evol **25:**2119–2128. http://dx.doi.org/10.1093/molbev/msn161.
56. **Langley S, Beveridge TJ**. 1999. Effect of O-side-chain-lipopolysaccharide chemistry on metal binding. Appl Environ Microbiol **65:**489–498.
57. **Boggis W, Kenward MA, Brown MR**. 1979. Effects of divalent metal cations in the growth medium upon sensitivity of batch-grown *Pseudomonas aeruginosa* to EDTA or polymyxin B. J Appl Bacteriol **47:**477–488. http://dx.doi.org/10.1111/j.1365-2672.1979.tb01209.x.
58. **Bird LJ, Coleman ML, Newman DK**. 2013. Iron and copper act synergistically to delay anaerobic growth of bacteria. Appl Environ Microbiol **79:**3619–3627. http://dx.doi.org/10.1128/AEM.03944-12.
59. **Dunning JC, Ma Y, Marquis RE**. 1998. Anaerobic killing of oral streptococci by reduced, transition metal cations. Appl Environ Microbiol **64:**27–33.
60. **Poulain AJ, Newman DK**. 2009. *Rhodobacter capsulatus* catalyzes light-dependent Fe(II) oxidation under anaerobic conditions as a potential detoxification mechanism. Appl Environ Microbiol **75:**6639–6646. http://dx.doi.org/10.1128/AEM.00054-09.
61. **Nikaido H, Vaara M**. 1985. Molecular basis of bacterial outer membrane permeability. Microbiol Rev **49:**1–32.
62. **Craig SA, Carpenter CD, Mey AR, Wyckoff EE, Payne SM**. 2011. Positive regulation of the *Vibrio cholerae* porin OmpT by iron and Fur. J Bacteriol **193:**6505–6511. http://dx.doi.org/10.1128/JB.05681-11.
63. **Kim AD, Graham DE, Seeholzer SH, Markham GD**. 2000. *S*-adenosylmethionine decarboxylase from the archaeon *Methanococcus jannaschii*: identification of a novel family of pyruvoyl enzymes. J Bacteriol **182:**6667–6672. http://dx.doi.org/10.1128/JB.182.23.6667-6672.2000.
64. **Lu ZJ, Markham GD**. 2007. Metal ion activation of *S*-adenosylmethionine decarboxylase reflects cation charge density. Biochemistry **46:**8172–8180. http://dx.doi.org/10.1021/bi6025962.
65. **Jung IL, Oh TJ, Kim IG**. 2003. Abnormal growth of polyamine-deficient *Escherichia coli* mutant is partially caused by oxidative stress-induced damage. Arch Biochem Biophys **418:**125–132. http://dx.doi.org/10.1016/j.abb.2003.08.003.
66. **Tkachenko AG, Nesterova LY**. 2003. Polyamines as modulators of gene expression under oxidative stress in *Escherichia coli*. Biochemistry **68:**850–856. http://dx.doi.org/10.1007/s002030100301.
67. **McPhee JB, Bains M, Winsor G, Lewenza S, Kwasnicka A, Brazas MD, Brinkman FS, Hancock RE**. 2006. Contribution of the PhoP-PhoQ and PmrA-PmrB two-component regulatory systems to Mg^{2+}-induced gene regulation in *Pseudomonas aeruginosa*. J Bacteriol **188:**3995–4006. http://dx.doi.org/10.1128/JB.00053-06.
68. **Morel F, Hering JG**. 1993. Principles and applications of aquatic chemistry. Wiley, New York, NY.
69. **de Castro AP, Fernandes Gda R, Franco OL**. 2014. Insights into novel antimicrobial compounds and antibiotic resistance genes from soil metagenomes. Front Microbiol **5:**489. http://dx.doi.org/10.3389/fmicb.2014.00489.
70. **Regeimbal J, Bardwell JC**. 2002. DsbB catalyzes disulfide bond formation de novo. J Biol Chem **277:**32706–32713. http://dx.doi.org/10.1074/jbc.M205433200.
71. **Wen Y, Feng J, Scott DR, Marcus EA, Sachs G**. 2007. The HP0165-HP0166 two-component system (ArsRS) regulates acid-induced expression of HP1186 α-carbonic anhydrase in *Helicobacter pylori* by activating the pH-dependent promoter. J Bacteriol **189:**2426–2434. http://dx.doi.org/10.1128/JB.01492-06.
72. **Beringer P**. 2001. The clinical use of colistin in patients with cystic fibrosis. Curr Opin Pulm Med **7:**434–440. http://dx.doi.org/10.1097/00063198-200111000-00013.
73. **Kopf SH, Henny C, Newman DK**. 2013. Ligand-enhanced abiotic iron oxidation and the effects of chemical versus biological iron cycling in anoxic environments. Environ Sci Technol **47:**2602–2611. http://dx.doi.org/10.1021/es3049459.
74. **Stookey LL**. 1970. Ferrozine---a new spectrophotometric reagent for iron. Anal Chem **42:**779–781. http://dx.doi.org/10.1021/ac60289a016.

75. **Lukat GS, McCleary WR, Stock AM, Stock JB**. 1992. Phosphorylation of bacterial response regulator proteins by low molecular weight phosphodonors. Proc Natl Acad Sci U S A **89:**718–722. http://dx.doi.org/10.1073/pnas.89.2.718.
76. **Bose A, Newman DK**. 2011. Regulation of the phototrophic iron oxidation (*pio*) genes in *Rhodopseudomonas palustris* TIE-1 is mediated by the global regulator, FixK. Mol Microbiol **79:**63–75. http://dx.doi.org/10.1111/j.1365-2958.2010.07430.x.
77. **Tatusov RL, Galperin MY, Natale DA, Koonin EV**. 2000. The COG database: a tool for genome-scale analysis of protein functions and evolution. Nucleic Acids Res **28:**33–36. http://dx.doi.org/10.1093/nar/28.1.33.
78. **Haft DH, Selengut JD, White O**. 2003. The TIGRFAMs database of protein families. Nucleic Acids Res **31:**371–373. http://dx.doi.org/10.1093/nar/gkg128.
79. **Finn RD, Bateman A, Clements J, Coggill P, Eberhardt RY, Eddy SR, Heger A, Hetherington K, Holm L, Mistry J, Sonnhammer EL, Tate J, Punta M**. 2014. Pfam: the protein families database. Nucleic Acids Res **42:**D222–D230. http://dx.doi.org/10.1093/nar/gkt1223.
80. **Marchler-Bauer A, Zheng C, Chitsaz F, Derbyshire MK, Geer LY, Geer RC, Gonzales NR, Gwadz M, Hurwitz DI, Lanczycki CJ, Lu F, Lu S, Marchler GH, Song JS, Thanki N, Yamashita RA, Zhang D, Bryant SH**. 2013. CDD: conserved domains and protein three-dimensional structure. Nucleic Acids Res **41:**D348–D352. http://dx.doi.org/10.1093/nar/gks1243.
81. **Altschul SF, Gish W, Miller W, Myers EW, Lipman DJ**. 1990. Basic local alignment search tool. J Mol Biol **215:**403–410. http://dx.doi.org/10.1016/S0022-2836(05)80360-2.
82. **Schultz J, Milpetz F, Bork P, Ponting CP**. 1998. SMART, a simple modular architecture research tool: identification of signaling domains. Proc Natl Acad Sci U S A **95:**5857–5864. http://dx.doi.org/10.1073/pnas.95.11.5857.
83. **Bolger AM, Lohse M, Usadel B**. 2014. Trimmomatic: a flexible trimmer for Illumina sequence data. Bioinformatics **30:**2114–2120. http://dx.doi.org/10.1093/bioinformatics/btu170.
84. **Langmead B, Trapnell C, Pop M, Salzberg SL**. 2009. Ultrafast and memory-efficient alignment of short DNA sequences to the human genome. Genome Biol **10:**R25. http://dx.doi.org/10.1186/gb-2009-10-3-r25.
85. **Li H, Handsaker B, Wysoker A, Fennell T, Ruan J, Homer N, Marth G, Abecasis G, Durbin R**, 1000 Genome Project Data Processing Subgroup. 2009. The sequence alignment/map format and SAMtools. Bioinformatics **25:**2078–2079. http://dx.doi.org/10.1093/bioinformatics/btp352.
86. **Delhomme N, Padioleau I, Furlong EE, Steinmetz LM**. 2012. easyRNASeq: a bioconductor package for processing RNA-Seq data. Bioinformatics **28:**2532–2533. http://dx.doi.org/10.1093/bioinformatics/bts477.
87. **Dietrich LE, Price-Whelan A, Petersen A, Whiteley M, Newman DK**. 2006. The phenazine pyocyanin is a terminal signalling factor in the quorum sensing network of *Pseudomonas aeruginosa*. Mol Microbiol **61:**1308–1321. http://dx.doi.org/10.1111/j.1365-2958.2006.05306.x.
88. **Koski P, Helander IM, Sarvas M, Vaara M**. 1987. Analysis of polyamines as their dabsyl derivatives by reversed-phase high-performance liquid chromatography. Anal Biochem **164:**261–266. http://dx.doi.org/10.1016/0003-2697(87)90395-2.